Comparative Evaluation of Control Techniques for a Three-Phase Three-Switch Buck-Type AC-to-DC PWM Converter System

Thomas Nussbaumer and Johann W. Kolar

Swiss Federal Institute of Technology (ETH) Zurich
Power Electronic Systems Laboratory
ETH Zentrum, ETL/H23
CH-8092 Zurich, Switzerland
Tel.: +41-1-632-6973 Tel.: +41-1-632-2834
email: nussbaumer@lem.ee.ethz.ch email: kolar@lem.ee.ethz.ch

Abstract — In this paper the cascade output voltage control of a unidirectional three-phase three-switch buck-type unity power factor PWM rectifier is discussed. Two control structures, i.e. an inner DC side inductor current control in combination with active input filter damping and an inner AC side input current and input filter capacitor voltage control are discussed. Guidelines for the control design which is based on a dynamically equivalent DC-to-DC converter model are given. Small signal transfer functions are derived by state space averaging. Finally, a comparative evaluation of the dynamics and of the realization effort of the control schemes is given and the continuation of the research is discussed.

Index Terms — Three-phase three-switch buck-type PWM rectifier, cascade control, dynamically equivalent DC-to-DC converter model, control design and evaluation.

I. INTRODUCTION

Three phase buck-type PWM rectifier systems (also known as current source rectifiers) are frequently employed as front-end converters in utility interfaced systems such as, e.g., power supplies in telecommunications and process technology, and AC drives. As compared to boost-type (voltage-source) topologies, the control design for current source topologies in general is more involved due to the higher system order which is caused by second order filtering on the AC and DC side.

On the other hand, current source rectifiers do provide a wide output voltage control range and do allow current limitation also in case of an output short circuit.

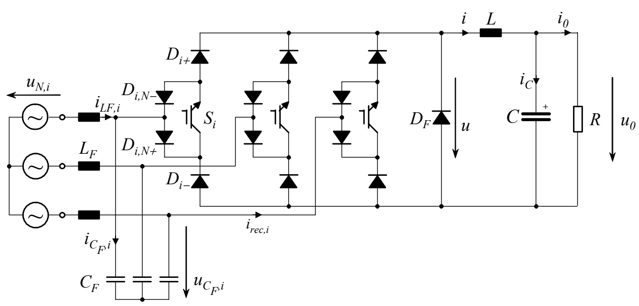

Fig. 1: Structure of the power circuit of the investigated three-phase three-switch AC-to-DC buck-type PWM rectifier.

In order to reduce the number of power transistors as compared to bidirectional current source systems a three-phase three-switch buck-type PWM rectifier topology has been developed in [1] (cf. **Fig. 1**). The control of this system to the knowledge of the authors so far has been treated in more detail only in [2] and [3] where an output voltage control in combination with an off-line PWM pattern generation scheme has been proposed. Apart from the fact, that the dynamics and the phase shift resulting from the input filter have been neglected, operation with off-line PWM patterns in general results in slow transient response of the output voltage control and in a potentially low input current quality and/or in input filter resonance problems [4]. This does give the motivation for a more detailed analysis of the system control.

In this paper, cascade output voltage control schemes which have been employed successfully for the bidirectional current source PWM converter and for the VIENNA Rectifier III [5] are adapted and comparatively evaluated for the three-switch rectifier.

For the bidirectional current source topology, usually an outer DC voltage or current control loop is employed to keep the output quantity at a constant value [6], [7], [8]. In order to form sinusoidal input currents two different concepts for the inner closed-loop control have been proposed:

1. Inner AC Current Control

When employing an AC current control (cf. **Fig. 2(a)**) the three input phase currents are controlled with high dynamics [9]. The templates for the current reference values are synchronized with the mains phase voltages in order to achieve ohmic fundamental mains behavior and/or unity power factor.

Due to the high order of the system to be controlled, the current loop bandwidth has to be selected well below the input filter resonance frequency, i.e. current control is not effective at the filter resonance. Furthermore, additional active or passive damping is required in order to effectively suppress input line current oscillations.

Therefore, in this paper an AC current control in combination with an underlying filter capacitor voltage control [6] is provided.

2. Inner DC Current Control

Inner DC current control (cf. **Fig. 2(b)**) has been applied to buck-type rectifier systems e.g. in [10] and [11]. There, no synchronization to the mains is required, but active input filter damping has to be provided in order to suppress filter oscillations which would result in input current distortion. The input current is only controlled in open loop in this case.

The above-mentioned control schemes will be analyzed and comparatively evaluated for a three-phase three-switch buck-type rectifier in the following. In **section 2** a linearized small signal model of the rectifier including the input filter is derived in order to analyze the control dynamics. Input filter damping concepts as proposed in the literature are discussed in **section 3** concerning damping performance and realization effort. In **section 4** the parameters of the control schemes are defined and in **section 5** the comparative evaluation of the closed loop performance is carried out by simulations. Finally, an outlook on the continuation of the research is given in **section 6**.

II. Control-Oriented Modeling

For analyzing the system dynamics as required for controller design the three-phase rectifier system can be transformed into an dynamically equivalent DC-to-DC converter with modified input stage variables. In [12] this concept has been proposed

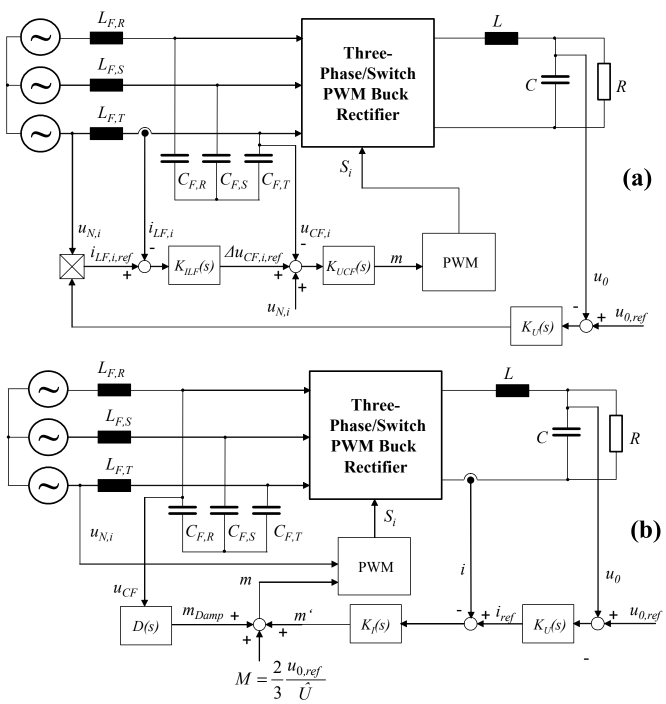

Fig. 2: Cascaded output voltage control schemes for a three-phase three-switch buck-type AC-to-DC converter as analyzed in this paper. **(a)** inner AC current control in combination with an underlying filter capacitor voltage control and a mains phase voltage pre-control; **(b)** inner DC current control in combination with input filter damping.

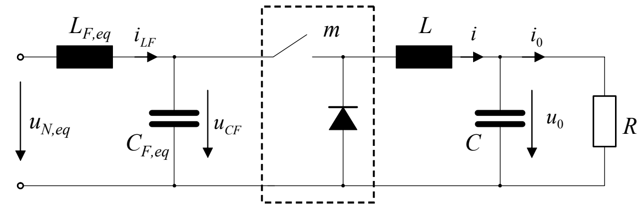

Fig. 3: Dynamically equivalent DC-to-DC converter model of the unidirectional three-phase three-switch AC-to-DC buck-type PWM rectifier.

for a three phase AC-to-DC boost converter. However, the basic transformation principle can also be applied to the buck topology, as within each 60°-wide interval of the mains period just two of the three rectifier bridge legs are active and the three-phase AC-to-DC converter can be modeled as two DC-to-DC converters operating in parallel and equally sharing the load. Hence, the rectifier can be viewed as a single DC-to-DC buck converter (cf. **Fig. 3**) with an equivalent input filter capacitor $C_{F,eq}$ and an equivalent input filter inductor $L_{F,eq}$

$$C_{F,eq} = \frac{2}{3} C_F \tag{1}$$

$$L_{F,eq} = \frac{3}{2} L_F \,. \tag{2}$$

The equivalent input voltage $u_{N,eq}$ for the equivalent DC-to-DC buck converter is obtained by considering the equality of the input power of the three-phase system and of the equivalent DC-to-DC converter system

$$u_{N,eq} = \frac{3}{2} \cdot \frac{\hat{U}_N \cdot \hat{I}_N}{i_{N,eq}} = \frac{3}{2} \hat{U}_N \,. \tag{3}$$

where

$$\hat{I}_N = i_{N,eq} \,. \tag{4}$$

is defined. According to Eq. (4) the modulation index of the three-phase system [5] and the duty-cycle of the equivalent DC-to-DC converter show equal values

$$m = \frac{\hat{I}_N}{i} = \frac{i_{N,eq}}{i} \,. \tag{5}$$

As verification of the physical meaning of the selection of the equivalent system parameters one could show that the amount of energy stored in the input filter inductors and/or input filter capacitors of both systems is equal

$$\begin{aligned} E_L &= \frac{1}{2} L_F \cdot \left(\hat{I}_N \cos(\omega t)\right)^2 + \frac{1}{2} L_F \cdot \left(\hat{I}_N \cos(\omega t - \frac{2\pi}{3})\right)^2 + \\ &+ \frac{1}{2} L_F \cdot \left(\hat{I}_N \cos(\omega t + \frac{2\pi}{3})\right)^2 = \\ &= \frac{3}{4} L_F \hat{I}_N^2 = \frac{1}{2} \cdot L_{eq} i_{N,eq}^2 = E_{L,eq} \end{aligned} \tag{6}$$

$$\begin{aligned} E_C &= \frac{1}{2} C_F \cdot \left(\hat{U}_N \cos(\omega t)\right)^2 + \frac{1}{2} C_F \cdot \left(\hat{U}_N \cos(\omega t - \frac{2\pi}{3})\right)^2 + \\ &+ \frac{1}{2} C_F \cdot \left(\hat{U}_N \cos(\omega t + \frac{2\pi}{3})\right)^2 = \\ &= \frac{3}{4} C_F \hat{U}_N^2 = \frac{1}{2} \cdot C_{eq} u_{N,eq}^2 = E_{C,eq} \end{aligned} \tag{7}$$

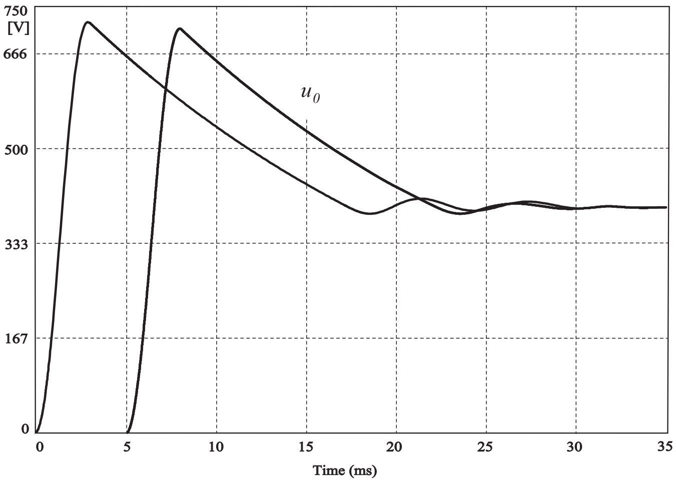

Fig. 4: Open loop start-up behavior of the equivalent DC-to-DC converter and of the three-phase buck-type PWM rectifier (starting with 5ms delay).

Also, an excellent matching of the behavior of the actual three-phase system and of the equivalent DC-to-DC converter can be proven by analyzing the open-loop start-up behavior of both systems (cf. **Fig 4)**.

In order to obtain a continuous state space model, state-space-averaging [13] can be utilized. There, the state equations for the turn-on and turn-off state of the switch have to be weighted with the corresponding relative on-times m and $1-m$ and then added line-by-line. Thereafter, in order to obtain the small-signal model, AC signal perturbations around an operating point are introduced. E.g. we then have for the modulation index

$$m = M + \tilde{m}\,. \tag{8}$$

By neglecting the products of perturbations the following linear small signal state-space model is obtained for the equivalent DC-to-DC converter

$$\begin{aligned}
\dot{\tilde{i}}_{LF} &= -\frac{1}{L_{F,eq}}\tilde{u}_{CF}\\
\dot{\tilde{u}}_{CF} &= \frac{1}{C_{F,eq}}(\tilde{i}_{LF} - M\tilde{i} - I_0\tilde{m})\\
\dot{\tilde{i}} &= \frac{1}{L}(M\tilde{u}_{CF} + U_{N,eq}\tilde{m} - \tilde{u}_0)\\
\dot{\tilde{u}}_0 &= \frac{1}{C}(\tilde{i} - \frac{1}{R}\tilde{u}_0).
\end{aligned} \tag{9}$$

A corresponding circuit is depicted in **Fig. 5**.

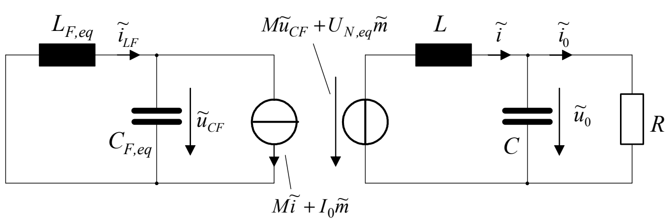

Fig. 5: Small signal model of the dynamically equivalent DC-to-DC buck converter.

III. Input Filter Damping

For the buck-type PWM converter an LC filter has to be inserted in between the mains and the converter input for attenuating switching frequency harmonics of the discontinuous rectifier input currents. Even if the resonance frequency of the LC filter is selected in a frequency band where no harmonics of the rectifier input current should exist, in practice harmonics of the supplying voltage could be amplified due to the filter resonance, whereby the filter could result in a steady state distortion of the input currents. In order to overcome this problem passive and/or active filter damping has to be provided, as discussed in the literature. Concepts which have been proposed include:

- introduction of damping resistors (passive damping) in parallel to the input filter inductors which, however, results in power losses [9]. In a practical system passive damping is required in any case for no-load operation of the rectifier. However, for analyzing the worst case condition damping resistors are not considered in this paper in the course of the control design.
- feedback and/or addition of the input filter inductor voltage $u_{LF} = u_N - u_{CF}$ to the input current reference signals in order to achieve a first order polynomial element in the denominator of the current control loop transfer function [14] . This solution does not take into account the inner inductance of the mains which could vary in a wide range and does take influence on the damping performance.
- insertion of a limitation of the maximum possible rate of rise of the current reference values [15]. This method is only effective on oscillations caused by the rectifier but could not damp oscillations resulting from mains voltage distortions.
- addition of a damping component
$$\tilde{m}_{Damp} = \tilde{u}_{CF} \cdot D(s) \tag{10}$$
to the modulation index reference value, where $D(s)$ is a high pass filtering function. This corresponds to introducing an equivalent damping resistor R_{eq}, which is only present for frequencies in the vicinity and above the filter resonance frequency [16], [17]. In comparison to the other damping schemes this method is very effective and is therefore utilized in the following for inner DC current control. The corner frequency of the high pass filter has to be positioned well below the input filter resonance frequency. For the system operating parameters given in the Appendix the damping has been defined as
$$D(s) = \frac{k \cdot T_D s}{1 + T_D s}\,. \tag{11}$$
with
$$T_D = 10^{-4} \qquad [s/rad]. \tag{12}$$
The effect of this damping for different values of the gain k is depicted in **Fig. 6** in a Bode diagram of the system to be controlled by the inner DC current control loop. **Figure 7** clearly shows that the damping scheme does results in a negative feedback of the integrator representing the input filter capacitor.

Remark: For the three-phase system oscillations of the input filter do result a changing magnitude and phase of the space vectors of the input filter inductor currents and input filter capacitor voltages. As a first step, in this paper only the amplitude of the filter capacitor voltage is used for the damping feedback, i.e. oscillations of the phase of the space vector are not taken into account what does result in non-uniform damping performance over the mains period. A further improvement and more detailed analysis of the damping scheme will be the topic of further investigations of the system control.

- Introduction of an input filter capacitor voltage control [17], [5] where the filter capacitor voltage reference value is defined by an input current control. Like active input filter damping (cf. **Fig 7**) this also does constitute a negative feedback path (for negative capacitor voltage controller gain, cf. **Fig. 13**).

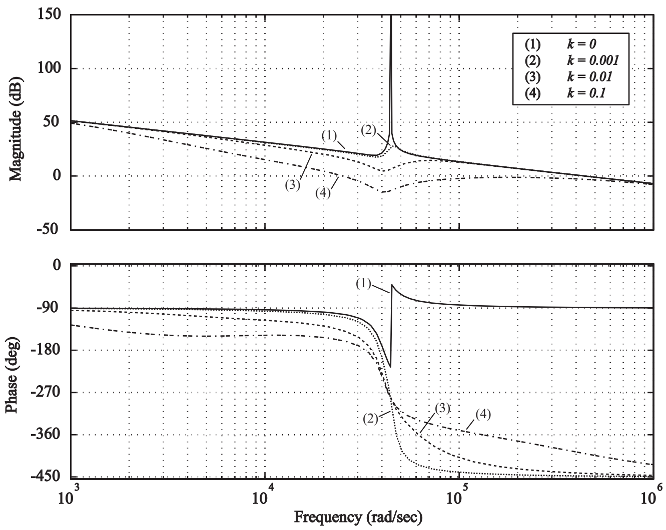

Fig. 6: Effects of input filter damping on the Bode diagram of the system to be controlled by the DC current controller for different values of the gain *k* [V^{-1}] of the damping transfer function *D(s)*.

IV. Controller Design

A. Inner DC current control

For designing the cascaded output voltage control with inner DC current control the linearized small-signal model of Eq. (9) in combination with the active damping

$$\tilde{m} = \tilde{m}' + \tilde{m}_{Damp}\,, \tag{13}$$

is considered where *m'* is the output of the current controller

$$\tilde{m}' = K_I(s)\cdot(\tilde{i}_{ref} - \tilde{i}\,)\,. \tag{14}$$

For designing the cascade control, first the inner loop is analyzed by neglecting the dynamics of the outer loop, i.e. for assuming u_0 as constant. For the design of the DC current controller the magnitude and the phase of the transfer function $G_I(s) = \tilde{i}/\tilde{m}$ is calculated as depicted in **Fig. 8** for different operating points (the rectifier operating parameters and component values are specified in the Appendix).

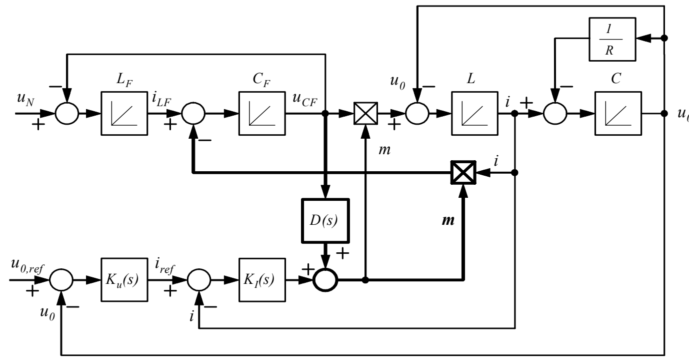

Fig. 7: Block diagram of the cascade output voltage control comprising an inner DC current control and active input filter damping. The bold line indicates the negative feedback providing active input filter damping.

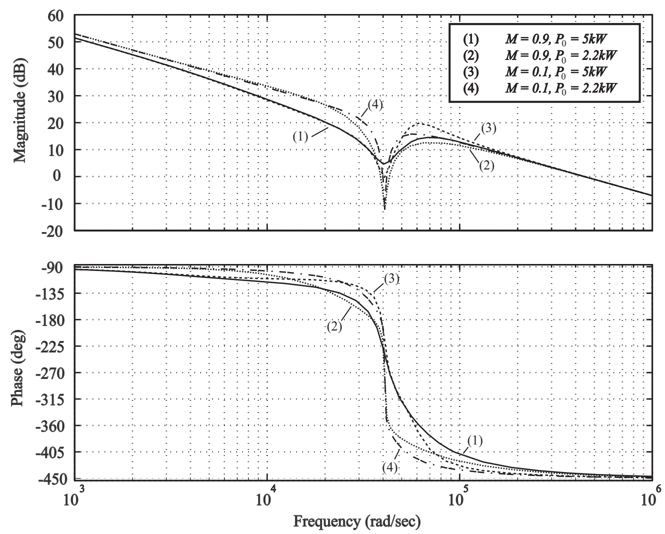

Fig. 8: Bode-diagram of the system to be controlled by the inner DC current $G_I(s)$ for different operating conditions.

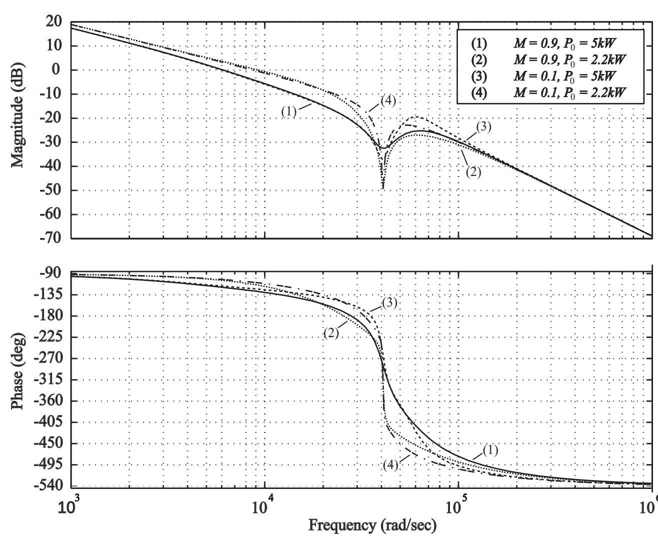

Fig. 9: Bode-diagram of the open loop transfer function $G_I(s)\cdot K_I(s)$ of the inner DC current control for different operating conditions.

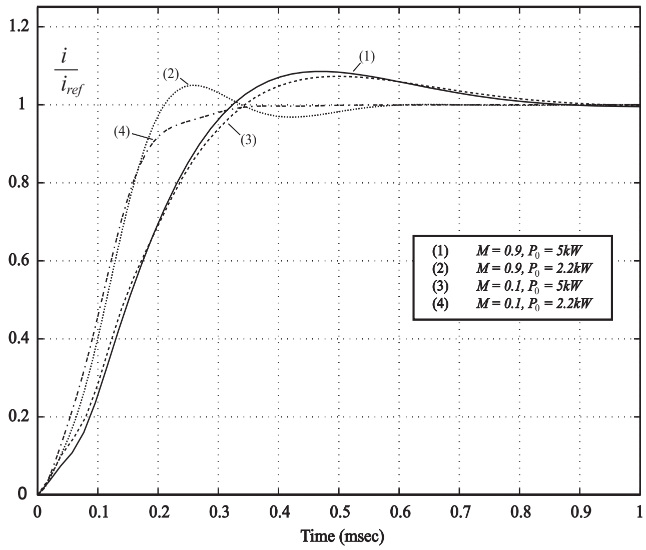

Fig. 10: Normalized step response of the inner DC current control for different operating points (normalization basis: i_{ref}).

For the design of an inner control loop primarily stability and dynamics are important. Accordingly, only a PT_1-type controller

$$K_I(s) = \frac{k_{P,I}}{1 + sT_1} \tag{15}$$

is provided in the case at hand. The controller gain is defined as

$$k_{P,I} = 0.02 \quad \left[A^{-1}\right] \tag{16}$$

with respect to ensuring enough phase margin, the first order lag element being characterized by

$$T_1 = 2.5 \cdot 10^{-5} \quad \left[s/rad\right] \tag{17}$$

keeps the magnitude of the transfer function at higher frequencies below 0dB for all operating points as depicted in **Fig. 9**. The control shows a good tracking performance for all operating points (cf. **Fig. 10**).

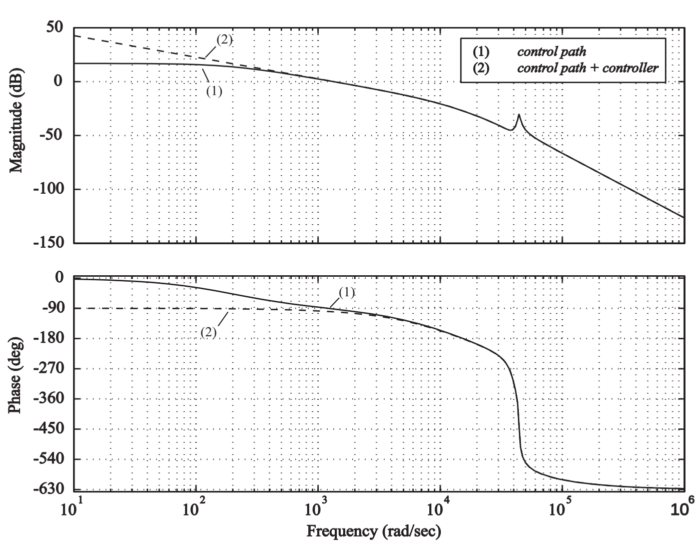

Fig. 11: Bode-diagram of the system to be controlled by the output voltage controller (control path $G_U(s)$) for inner DC current control **(1)** and open loop transfer function $G_U(s) \cdot K_U(s)$ **(2)**.

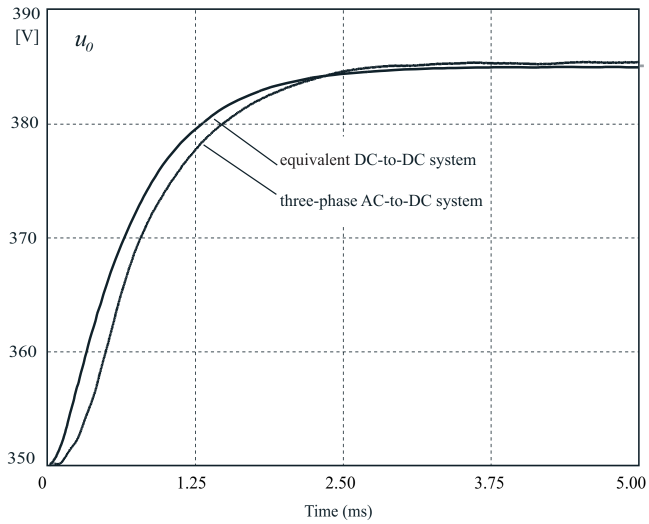

Fig. 12: Step response of the output voltage control of the dynamically equivalent DC-to-DC converter and of the actual three-phase PWM rectifier system for a reference step of 10% when employing an inner DC current control and active input filter damping.

Subsequent to a successful inner control loop control design the resulting control equation

$$\tilde{m} = K_I(s) \cdot (\tilde{i}_{ref} - \tilde{i}\,) + \tilde{u}_{CF} \cdot D(s)\,, \tag{18}$$

has to be added to the state-space model of Eq. (9). The design of the outer voltage controller $K_U(s)$ now can be based on the Bode-diagram of the transfer function

$$G_U(s) = \tilde{u}_0 / \tilde{i} \ . \tag{19}$$

(cf. **Fig. 11**) where stability and stationary control accuracy are relevant. Furthermore, in the case at hand no overshoot of the output voltage step response can be accepted. According to the resulting Bode-diagram (cf. **Fig. 11**) a simple PI-type controller

$$K_U(s) = k_{P,U} + \frac{1}{sT_U} \tag{20}$$

can be employed (cf. **Fig. 11**). The integral component of the controller does provide large low frequency gain, the gain $k_{P,U}$ defines the unity gain frequency. For ensuring enough phase margin we select

$$\begin{aligned} k_{P,U} &= 1 \quad [A/V] \\ T_U &= 0.005 \quad [s/rad] \end{aligned} \tag{21}$$

As verified by the step response for a reference step of 10% depicted in **Fig. 12** the control shows a good tracking performance without overshoot. This also holds for applying the control to the three-phase system (cf. **Fig. 12**).

B. Inner AC current control

The control design for inner AC current control can be carried out in an analogous manner as described for inner DC current control.

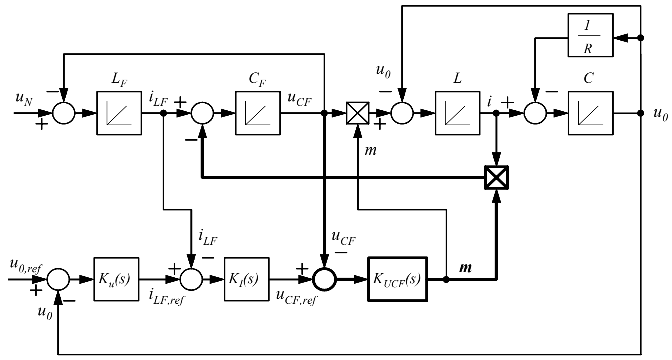

Fig. 13: Block diagram of the system control with inner AC current control in combination with underlying input filter capacitor voltage control. The bold line indicates the negative feedback path providing input filter damping.

For input filter damping an underlying filter capacitor voltage control is provided (cf. **Fig. 13**), where the filter capacitor voltage controller has to be designed for the control path

$$G_{UCF}(s) = \tilde{u}_{CF} / \tilde{m} \tag{22}$$

Since the control path shows a negative gain, an inverting controller has to be implemented. The unity gain frequency is set well below the switching frequency and a first order delay is added in order to attenuate switching frequency components contained in the filter capacitor voltage.

With reference to the Bode-diagram shown in **Fig. 14** the parameters of the PT_1-type controller

$$K_{UCF}(s) = \frac{k_{P,UCF}}{1 + sT_{UCF}} \tag{23}$$

have been selected as

$$\begin{aligned} k_{P,UCF} &= -0.013 \quad \left[V^{-1}\right] \\ T_{UCF} &= 5 \cdot 10^{-6} \quad \left[s / rad\right] \end{aligned} \tag{24}$$

The resulting step response of the filter capacitor voltage control is depicted in **Fig. 15**.

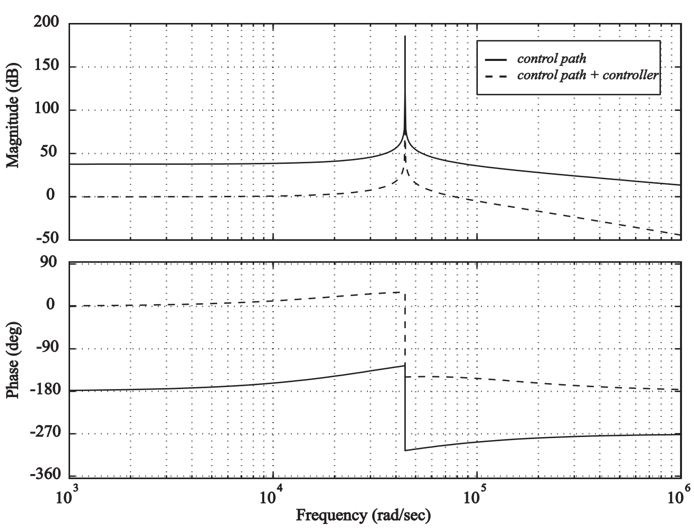

Fig. 14: Bode-diagram of the system to be controlled by the filter capacitor voltage control (control path $G_{UCF}(s)$) and open loop transfer function $G_{UCF}(s) \cdot K_{UCF}(s)$.

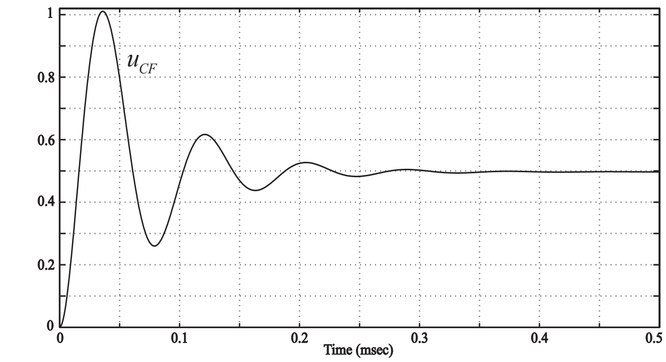

Fig. 15: Step response of the filter capacitor voltage control.

For the design of the filter inductor current controller the control path

$$G_{ILF}(s) = \tilde{i}_{LF} / \tilde{u}_{CF,ref} \ , \tag{25}$$

including the dynamics of the filter capacitor voltage control, has to be analyzed. In order to obtain a unity gain angular frequency of $5 \cdot 10^4 rad/s$ a P-type controller

$$K_{ILF}(s) = k_{P,ILF} \tag{26}$$

with

$$k_{P,UCF} = -10 \quad \left[V / A\right] \tag{27}$$

is sufficient (cf. **Fig. 16**).

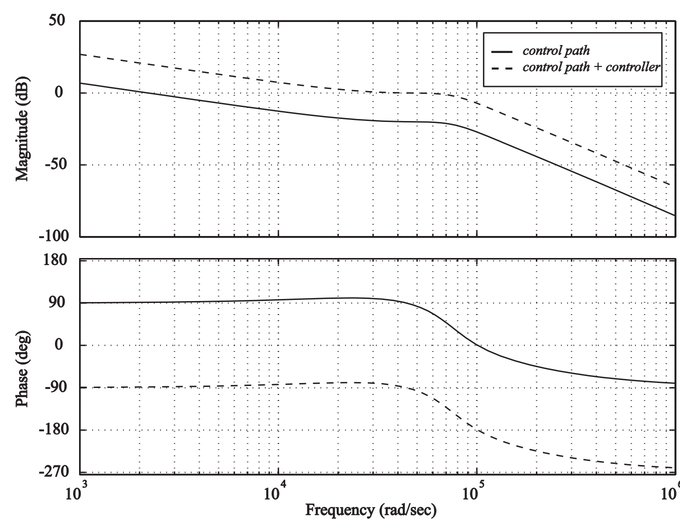

Fig. 16: Bode-diagram of the system to be controlled by the output voltage control (control path $G_{ILF}(s)$) and open loop transfer function $G_{ILF}(s) \cdot K_{ILF}(s)$.

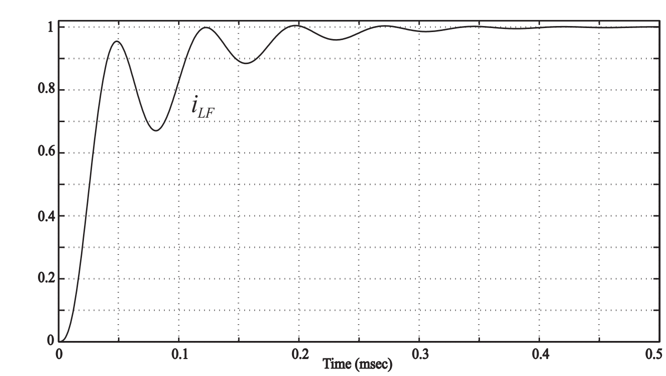

Fig. 17: Step response of the filter inductor current control.

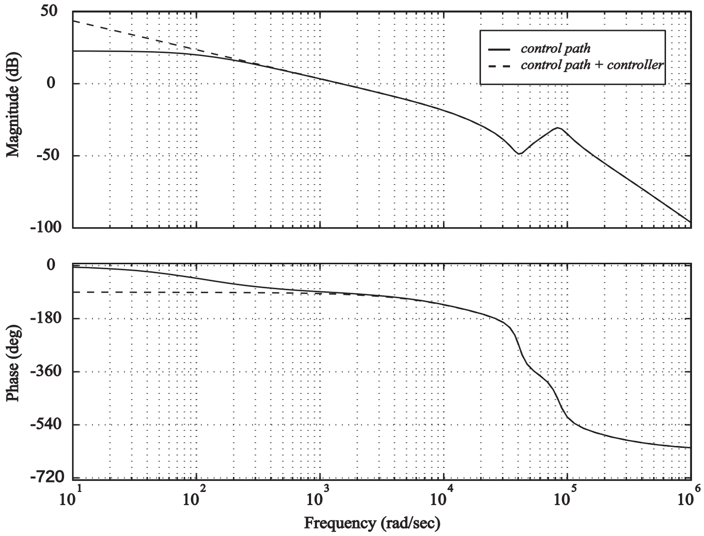

Fig. 18: Bode-diagram of the system to be controlled by the output voltage controller (control path $G_U(s)$ for inner AC current control in comparison to the open loop transfer function $G_U(s) \cdot K_U(s)$.

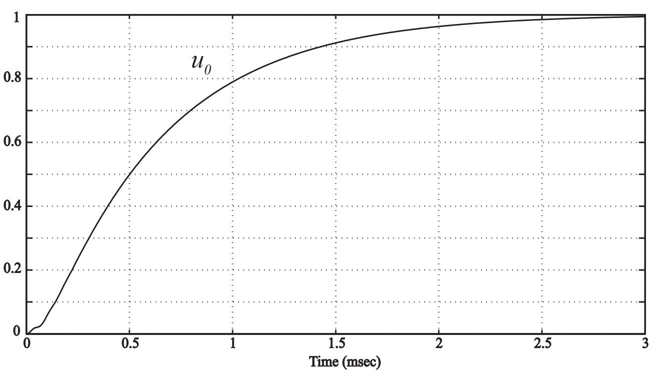

Fig. 19: Step response of the output voltage control.

The resulting step response of the closed filter inductor current control loop is depicted in **Fig. 17**.

Finally, as for the inner DC current control a PI-type controller is selected for the outer output voltage control (cf. **Fig. 18**)

$$\begin{aligned} k_{P,U} &= 1 \quad [A/V] \\ T_1 &= 0.09 \quad s/rad \end{aligned}. \tag{28}$$

The resulting step response of the closed loop is depicted in **Fig. 19**.

V. Performance Comparison

For the comparative evaluation of the performance of the two control concepts the response to an

- output voltage reference step of 10% starting from $u_0 = 350V$, to a
- step of the input voltage amplitude $\hat{U}$ of 10% of the rated value occurring simultaneously for all phases, and to a
- step of the load current i_0 of -25% of the rated value

is considered. As in practice usually the rate of change of a quantity is limited an overshoot resulting for a quantity controlled by an inner loop controller is not considered as disadvantage of a control concept.

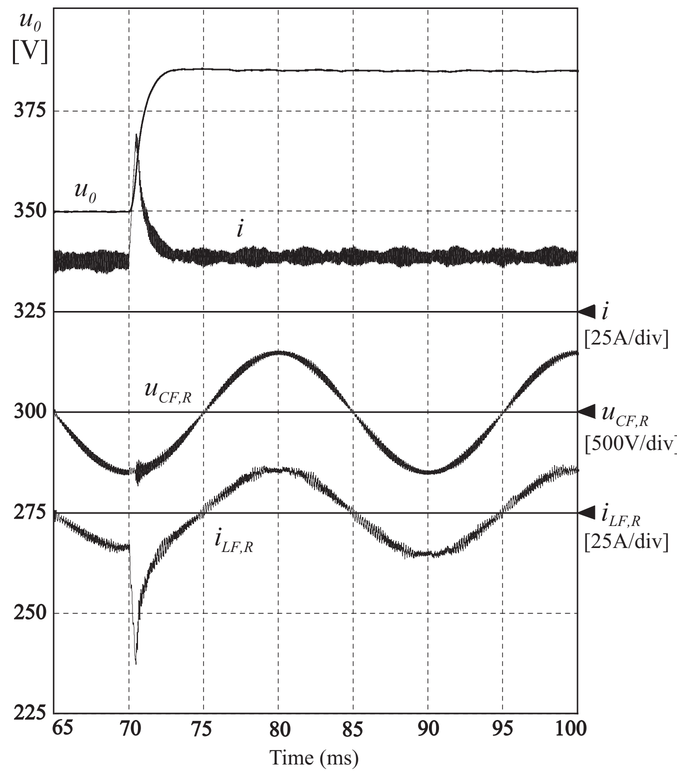

Fig. 20: Time behavior of output voltage u_0, DC inductor current i, input filter capacitor voltage $u_{CF,R}$ (phase R) and the input filter inductor current $i_{LF,R}$ (phase R) for an output voltage reference step of 10% at t=70ms when employing inner DC current control (vertical scale related to $\boldsymbol{u_O}$, scales of other quantities shown in brackets).

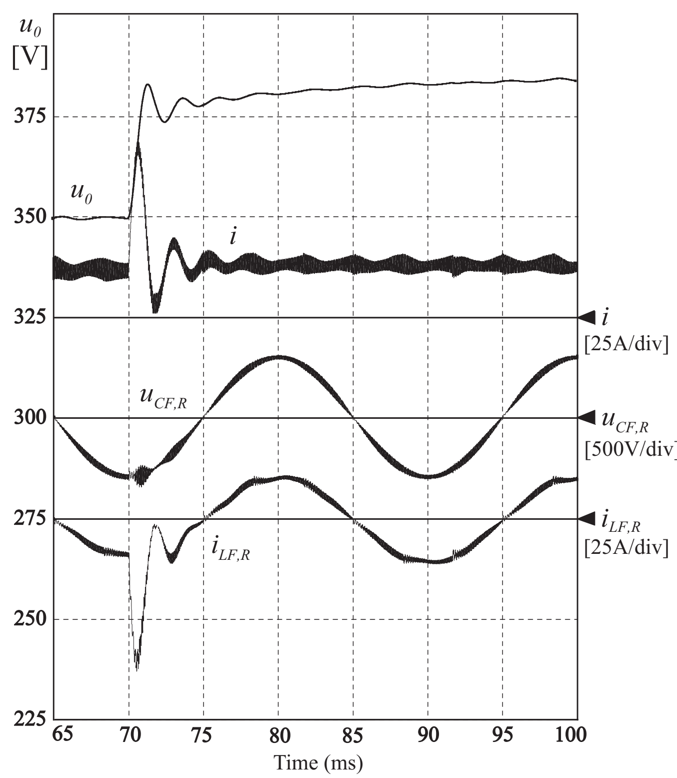

Fig. 21: As Fig. 20 but for inner AC current control.

As can be seen from **Figs. 20** and **21** the inner DC current control exhibits a better output voltage tracking as compared to inner AC current control.

Also, for a step-like increase of the input voltage amplitude (cf. **Figs. 22** and **23**) the output voltage tracking performance is surprisingly not better for inner AC current control.

A load step is handled by both controllers without any problems (cf. **Figs. 24** and **25**).

In summary, the DC current control shows a better output voltage tracking performance and a better disturbance reaction. Therefore, the larger realization effort of the inner AC side current control cannot be justified by improved dynamic behavior.

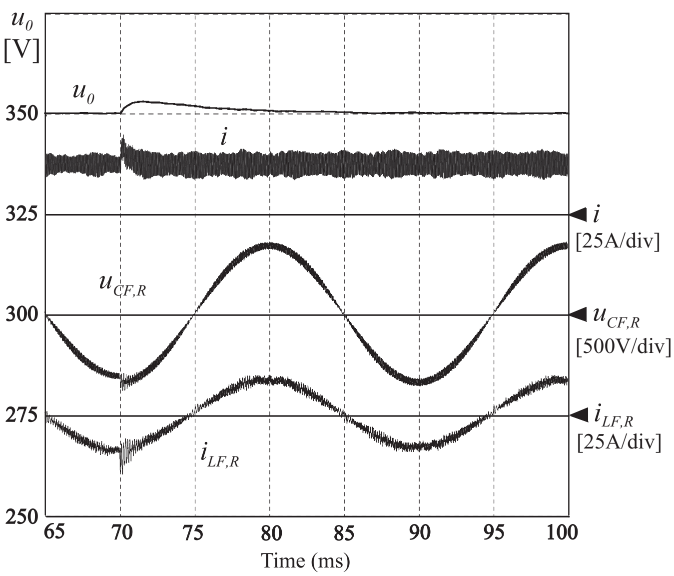

Fig. 22: Time behavior of output voltage u_0, DC inductor current i, input filter capacitor voltage $u_{CF,R}$ (phase R) and the input filter inductor current $i_{LF,R}$ (phase R) for a step of the input voltage amplitude $\hat{U}$ of 10% at $t=70ms$ when employing inner DC current control (vertical scale related to $\boldsymbol{u_O}$, scales of other quantities shown in brackets).

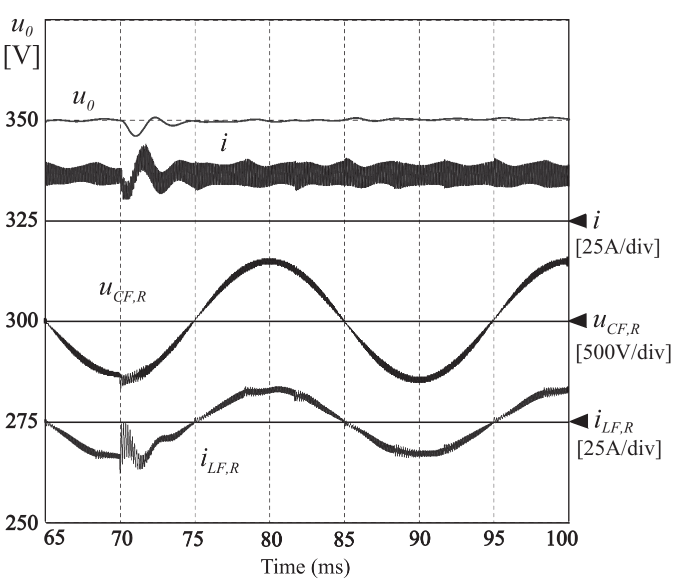

Fig. 23: As Fig. 22 but for inner AC current control.

VI. Continuation of Research

In a next step the controller dimensioning performed in this paper by digital simulations will be verified on a 5kW prototype of the system. There, the control behavior also will be studied for a constant power load, for mains voltage asymmetries, and for large signal disturbances.

Furthermore, the damping for inner DC current control which has been based on the magnitude of the space vector of the filter capacitor voltages in the case at hand will be analyzed in more detail and extended in order to also accommodate space vector phase oscillations.

Finally, novel control structures as, e.g. a cascaded state-space control will be investigated.

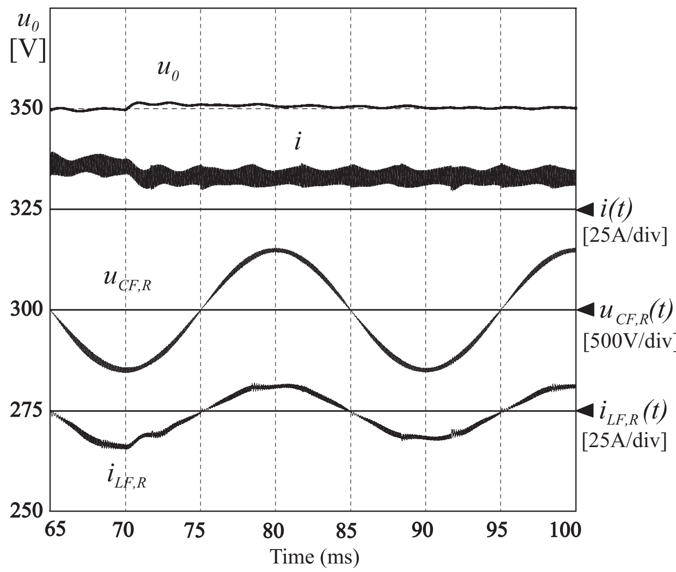

Fig. 24: Time behavior of output voltage u_0, DC inductor current i, input filter capacitor voltage $u_{CF,R}$ (phase R) and the input filter inductor current $i_{LF,R}$ (phase R) for a load step of -25% at t=70ms when employing inner DC current control (vertical scale related to $\boldsymbol{u_O}$, scales of other quantities shown in brackets).

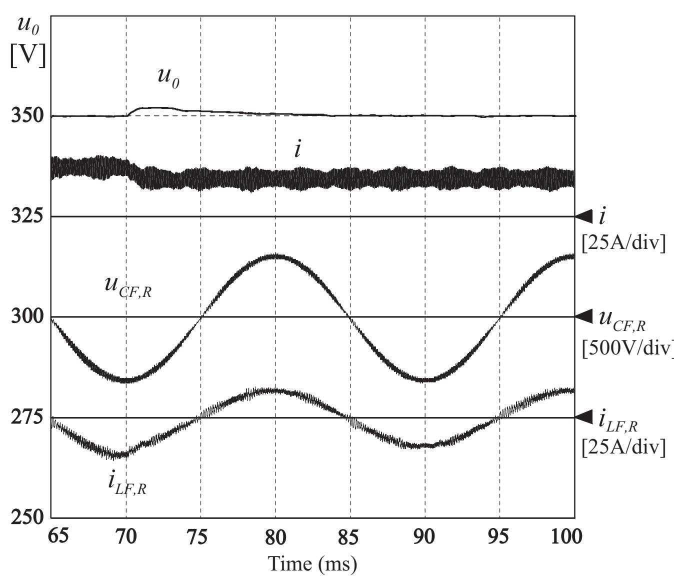

Fig. 25: As Fig.22 but for inner AC current control.

APPENDIX

System operating parameters:

$$\begin{array}{ll} P_0 = 5kW & \text{(rated output power)} \\ \hat{U}_N = 300V & M = 0.9 \\ L_F = 150\mu H & U_0 = 400V \\ C_F = 4\mu F & L = 1mH \\ I_0 = 12.5A & C = 750\mu F \end{array} .$$

REFERENCES

[1] **L. Malesani, P. Tenti**, "Three-Phase AC/DC PWM Converter with Sinusoidal AC Currents and Minimum Filter Requirements", *IEEE Trans. Ind. App. 1987,vol. IA-23, no. 1, pp. 71-77.*

[2] **R. Itoh**, "Steady-State and Transient Characteristics of a Single-Way Step-Down PWM GTO Voltage-Source Converter with Sinusoidal Supply Currents", *IEE Proc., Electr. Power Appl., 1989, vol. B, no. 4, pp. 168-174.*

[3] **T. Grossen, E. Menzel and J.H.R. Enslin**, "Three-Phase Buck Active Rectifier with Power Factor Correction and Low EMI", *IEE Proc., 1999, vol. B, no. 5, pp. 591-596.*

[4] **J. Espinoza, G. Joós**, "On-line Generation of Gating Signals for Current Source Converter Topologies", *Conf. Rec. IEEE-ISIE 1993, pp. 674-678.*

[5] **J.W. Kolar, U. Drofenik, H. Ertl, F.C. Zach,** „VIENNA Rectifier III – A Novel Three-Phase Single-Stage Buck-Derived Unity Power Factor AC-to-DC Converter System", *Proc. of the Nordic Workshop on Power and Industrial Electronics, pp. 9-18.*

[6] **A. Mechi, S. Funabiki**, "Three-Phase PWM AC-to-DC Converter with a Wide Control Range of DC Voltage", *IEE Trans. Japan, 1994, vol. 114-D, no. 6, pp. 638-646.*

[7] **Y. Sato, T. Kataoka**, "State Feedback Control of Current-Type PWM AC-to-DC Converters", *Conf. Rec. IEEE-IAS 1991, pp. 840-846.*

[8] **X. Wang, B.T. Ooi**, "Real-Time Multi-DSP Control of three phase Current-Source Unity Power Factor PWM Rectifier", *Conf. Rec. IEEE-PESC 1992, pp. 1376-1383.*

[9] **N.R. Zargari, G. Joós**, "A Current Controlled Current Source Type Unity Power Factor PWM Rectifier", *Conf. Rec. IEEE-IAS 1993, pp. 793-799.*

[10] **D.J. Tooth**, "The Behaviour and Analysis of a Three-Phase AC-DC Step-Down Unity Power Factor Converter", *Ph.D. Dissertation, Dept. of Computing and Electr. Eng., Heriot-Watt University, Scotland, 1999.*

[11] **M. Baumann, J.W. Kolar**, "Experimental Analysis of a 5kW Wide Input Voltage Range Three-Phase Buck+Boost Power Factor Corrector", *Conf. Rec. IEEE-INTELEC 2001, pp. 146-153.*

[12] **H. Mao, D. Boroyevich, F.C. Lee**, "Novel Reduced-Order Small-Signal Model of a Three-Phase PWM Rectifier and Its Application in Control Design and System Analysis", *IEEE Trans. Power Elec., 1998, vol. 3, pp. 511-521.*

[13] **R.D. Middlebrook**, and S. Cuk, "A General Unified Approach to Modeling Switching Converter Power Stages", *Conf. Rec. IEEE-PESC 1976, pp.18-34.*

[14] **G.D. Marques**, "A PWM Rectifier Control System with DC Current Control based on the Space Vector Modulation and AC Stabilisation", *Conf. Rec. IEEE-ISIE 1997, pp. 318-322.*

[15] **K. Toyama, T. Takeshita, N. Matsui**, "Transient Oscillation Suppression of Input Filter Voltage and Current for Current-Source Three-Phase PWM AC/DC Converter", *Conf. Rec. of Power Conversion Conf. 1997, pp. 253-258.*

[16] **L. Malesani, L. Rossetto, and P. Tenti**, "Active Power Filter with Hybrid Energy Storage", *IEEE Trans. Power Elec., 1991, vol. 6, no. 3, pp. 392-397.*

[17] **M. Baumann, U. Drofenik, J.W. Kolar**, "New Wide Input Voltage Range Three-Phase Unity Power Factor Rectifier Formed by Integration of a Three-Switch Buck-Derived Front-End and a DC/DC Boost Converter Output Stage", *Conf. Rec. IEEE-INTELEC 2000, pp. 461-470.*

[18] **Y. Sato, and T. Kataoka**, "A Current Type PWM Rectifier with Active Damping Function, *Conf. Rec. IEEE-IAS 1995, pp. 2333-2340.*